Combined Multidimensional Signaling and Transmit Diversity for High-Rate Wide-Band CDMA

Dong In Kim, *Member, IEEE,* and Vijay K. Bhargava, *Fellow, IEEE*

***Abstract*—Multidimensional signaling is newly designed to provide a diversity gain of order 2 using two transmit antennas in uplink transmission of wide-band CDMA (W-CDMA) while achieving high and multiple data rates at the same time. The rate can be easily changed on the slot basis in a frame transmission by adapting the order of multidimensional signaling to the incoming traffics. The multidimensional signaling of order zero simply reduces to conventional multicode scheme, so there exists a tradeoff between rate and complexity. Also, the use of multidimensional signaling results in far reduced envelope variations at the maximum rate. With the transmit diversity, the uplink signal-to-interference ratio (SIR) will be further stabilized to meet the requirements of multimedia traffics. Statistics of interferences are characterized in terms of their second- and fourth-order moments from which diversity gain is theoretically verified. For realistic multipath fading channels, considering both equal and unequal average path powers, the average probability of symbol error is obtained in compact form, in which the two schemes, multidimensional signaling with and without transmit diversity are compared, and then with nonmulticode scheme in view of the bit error rate (BER). Numerical and simulation results show that the multidimensional signal with transmit diversity provides a significant gain over that with no diversity, and furthermore outperforms nonmulticode scheme subject to the same signal energy per bit and chip rate.**

***Index Terms*—Diversity gain, multidimensional signaling, multicode DS-CDMA, two-branch transmit diversity.**

I. Introduction

In WIRELESS communications, much attention has been focused on increasing the data rate while maintaining link quality reliably. In particular, it is difficult to achieve this in the presence of multipath fading because the scheme with no diversity often requires a large increase in signal-to-noise ratio (SNR) even for a small reduction in the BER. Recently, there have been a number of proposals to deploy multiple transmit antennas at both the base and remote stations and increase the data rate of wireless channels. These proposals are basically based on antenna diversity, coding technique, and array processing. For instance, the space–time coding [1] introduces temporal and spatial correlation into signals transmitted from different antennas, which provides diversity and coding gain at the receiver. This coding technique is combined with the array processing at the receiver to provide reliable and very high data rate communication [2].

On the other hand, due to the power limitation as well as the cost and size of the remote units, the antenna diversity has almost exclusively been used at the base stations to improve the capacity of wireless channels. In particular, down link capacity can be effectively increased by employing the transmit diversity proposed in [3] and [4]. The approach introduces different delays in transmission at each antenna so that delayed versions of a signal experience independent fadings to provide diversity gain at the receiver. Another approach proposed in [5] is to achieve a simple diversity order of 2 when two transmit antennas with one receive antenna are used, in which the encoding is done in space and time (space–time coding). The delay diversity and coding schemes have been proposed mainly for use in narrow-band signals, while the diversity scheme in [6] was proposed for spread-spectrum signals using a RAKE receiver, but its use is limited to indoor wireless channels with very small delay spreads. A recent progress in transmit diversity for wide-band CDMA (W-CDMA) has been reported in [7] and [8], especially for a capacity increase in downlink.

In view of signal design, there have been two typical types of signaling to provide high data rate communication over wide-band wireless channels, i.e., the multicarrier code-division multiple-access (MC-CDMA) [9] and multicode direct-sequence CDMA (DS-CDMA) [10], [11]. The two CDMA techniques are being considered for use in downlink and uplink of the third-generation cellular systems in which the former is more suitable for synchronous channels but the latter is appropriate for asynchronous channels. The major problem with using the CDMA techniques is the envelope variations[1] as a result of large linear sum of parallel channels, and the interferences caused by nonorthogonal[2] other user signals. In uplink transmission, it is desirable to adopt a cost-effective nonlinear amplifier at the remote unit, and hence a signal suffers from the nonlinear distortions whenever large envelope variations occur. With a limitation on the peak-to-average envelope ratio, it is difficult to increase data rates simply by increasing the number of parallel channels for the CDMA schemes. In addition, the users with high data rates will create large interferences compared to the low-rate users because many parallel channels are used, and then it is required to increase the signal power of

Paper approved by M. Brandt-Pearce, the Editor for Modulation and Signal Design of the IEEE Communications Society. Manuscript received November 2, 1999; revised January 29, 2001. This work was supported in part by the Research Fund of the University of Seoul, Seoul, Korea, and in part by Natural Sciences and Engineering Research Council of Canada.

D. I. Kim is with the Department of Electrical and Computer Engineering, The University of Seoul, Seoul 130-743, Korea (e-mail: dikim@uoscc.uos.ac.kr).

V. K. Bhargava is with the Department of Electrical and Computer Engineering, University of Victoria, Victoria, BC V8W 3P6, Canada (e-mail: bhargava@ece.uvic.ca).

Publisher Item Identifier S 0090-6778(02)01361-2.

[1]We may avoid the problem with envelope variations by reducing the spreading factor to increase data rates [12].

[2]This results from the signals with distinct delays and/or the use of nonorthogonal codes.

low-rate users and also increase the interferences, which may require a certain degree of diversity gain for the high-rate users to overcome this unfavorable situation.

In this paper, we propose a multidimensional W-CDMA signaling combined with transmit diversity, in which the multidimensional W-CDMA signal is designed in order to avoid the problem with envelope variations when higher data rates are needed in uplink transmission, and the transmit diversity is adopted to obtain diversity gain by stabilizing the uplink SIR of high-rate users. Due to the limitations on the cost, size, and power of the remote units, it is desirable to use a simple two-branch transmit diversity [5] in which the delay diversity scheme [4] is used to have uncorrelated received signals from the two antennas. Here, if a signal and a delayed signal (more than one symbol period) are encoded by a user-specific signature sequence varying from symbol to symbol, we may have no intersymbol interference (ISI) at the receiver. Besides, the path gain averaged over a fading depends on the relative delay over many symbol periods, and, if delay versions of a signal pass through the multipath fading channel, their path gains with the same relative delays become uncorrelated and are varying instantly while the averaged path gains versus relative delays, called multipath intensity profile [13], would not be changed over several symbol periods.

High and multiple data rates are important for reliable wireless multimedia communications. In particular, it is necessary to adapt the rates according to the incoming traffics without causing extra hardware complexity at the remote units. For this reason, the proposed multidimensional W-CDMA signal is designed to easily change the rates by adapting the order of multidimensional signaling to the traffics with varying rates while the number of parallel channels is kept the same. A rate adaptation can be operated on the slot basis in a frame transmission of a W-CDMA uplink, and the change in rate may be detected together with data detection at the receiver because of signaling characteristics. Therefore, a newly designed W-CDMA signal with transmit diversity will be a good alternative to the MC-CDMA and multicode DS-CDMA with applications to next-generation wireless systems.

In Section II, the signal structure and characteristics of multidimensional W-CDMA signaling are described and a new signal design method is given both in code and time spaces. The multidimensional signaling is applied to provide a diversity order of 2 with two transmit antennas and one receive antenna in Section III, in which diversity gain is theoretically verified. Section IV derives the compact-form formula to calculate the probability of symbol error for the signaling with or without transmit diversity, in which a precoding is used to achieve a constant envelope signal, considering both equal and unequal average path powers. Section V presents numerical results to prove the diversity gain of order 2 and simulation results to compare the two schemes with nonmulticode scheme in terms of the BER. Finally, concluding remarks are given in Section VI.

II. Multidimensional W-CDMA Model

We consider multiple parallel transmissions using the orthogonal codes that are shared among all users in the uplink channel of W-CDMA systems, where a user-specific signature sequence concatenates them in order to discriminate his own transmission from others. Hence, the resulting waveform of a particular kth user can be expressed by

$$\tilde{s}_k(t) = \sqrt{P}\left[\sum_{m=0}^{M-1}\left[d_{I,m}^{(k)}(t) + jd_{Q,m}^{(k)}(t)\right]w_m(t)\right]c_k(t) \quad (1)$$

in which P is the transmit power per (code) channel, M is the number of parallel (code) channels, the in-phase (I) and quadrature (Q) parallel data are

$$d_{A,m}^{(k)}(t) = \sum_{n=0}^{N_f-1} d_{A,m}^{(k)}(n)p_T(t-nT) \quad (2)$$

for $d_{A,m}^{(k)}(n) \in \{1,-1\}$ $(A = I, Q)$, $p_T(t)$ denotes a unit-magnitude rectangular pulse occupied in $[0,T)$ for the symbol time T, and N_fT indicates the frame length. Here, the mth orthogonal code waveform $w_m(t)$ is of the form

$$w_m(t) = \sum_{i=0}^{GN_f-1}\sum_{l=0}^{M-1} w_{m,l}p_{T_c}(t-lT_c-iT_w) \quad (3)$$

in which the channelization codes $\{w_{m,l}\}$ are repeated G times per symbol to provide the degree of freedom $G \triangleq T/T_w$ (G is assumed to be an integer) in time space with M in code space, T_w and T_c denote Walsh symbol and chip times, respectively, and the row vector $\mathbf{w}_m \triangleq (w_{m,0},\ldots,w_{m,M-1})$ is chosen from the Hadamard matrix H_M generated by

$$H_l = \begin{pmatrix} H_{l/2} & H_{l/2} \\ H_{l/2} & -H_{l/2} \end{pmatrix} \quad (4)$$

with $l = 2,4,\ldots,M$ and $H_1 = 1$. Finally, the kth user signature waveform is modeled as

$$c_k(t) = \sum_{l=0}^{GMN_f-1} c_l^{(k)}p_{T_c}(t-lT_c) \quad (5)$$

where $N \triangleq GM$ represents the total degree of freedom in signal space or means the spreading factor, and $\{c_l^{(k)}\}$[3] may be obtained by shortening the long PN sequence of values ± 1 to the length of NN_f.

The above signaling structure can be viewed as a kind of multicode DS-CDMA that has been proposed by the literatures [10], [11], and partly employed in the W-CDMA uplink channel [12]. In this paper, we propose a novel multidimensional W-CDMA signaling based on this structure which enables us to convey more traffic and easily adapt to the multiple data rates of incoming traffics. It can be achieved by exploiting the addressing part of signature sequences as one of data modulation as shown in Fig. 1(a), which is formulated as

$$\tilde{s}_k(t) = \sqrt{P}\sum_{m=0}^{M-1}\left[d_{I,m}^{(k)}(t)c_{I,\langle m\rangle}^{(k)}(t) + jd_{Q,m}^{(k)}(t)c_{Q,\langle m\rangle}^{(k)}(t)\right]w_m(t) \quad (6)$$

[3]For simplicity, we take the real binary sequences, but it can be generalized to the case of complex spreading [12].

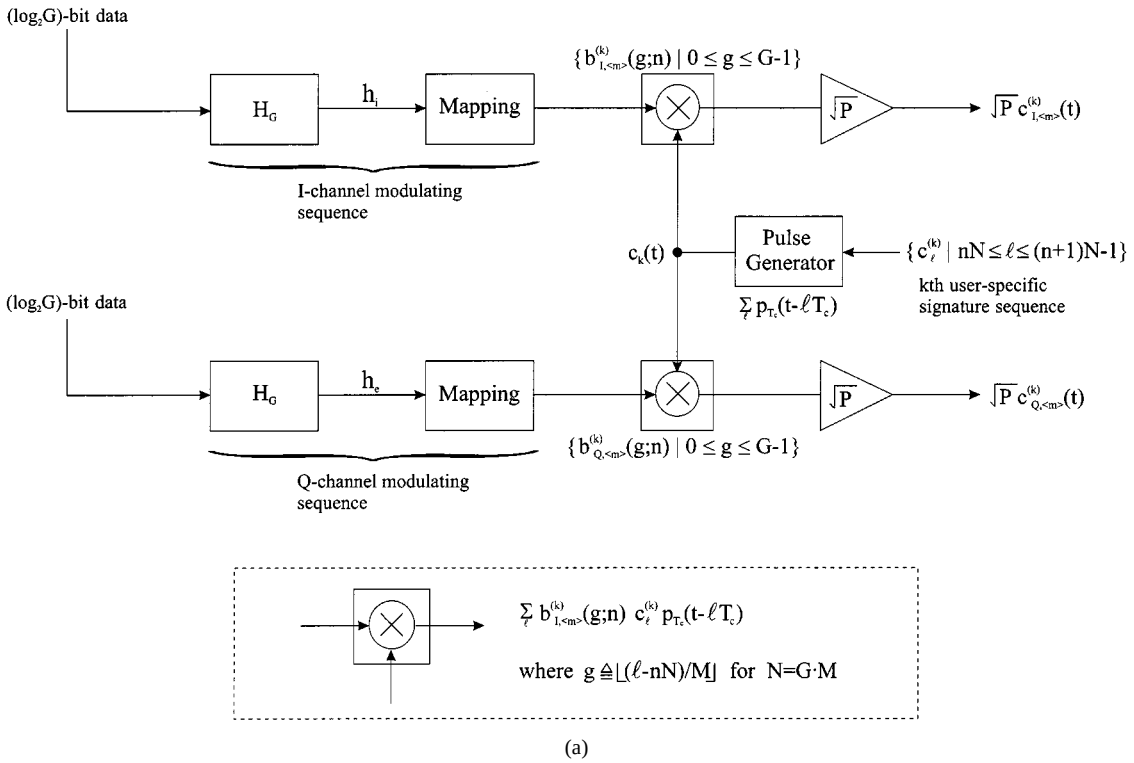

(a)

Fig. 1. Uplink W-CDMA system by the kth user's multidimensional signaling based on I- and Q-channel modulating sequences. (a) Data-modulated I- and Q-channel signature waveforms.

for $\langle m \rangle \triangleq \lfloor m/J \rfloor$ ($\lfloor x \rfloor$ denotes the greatest integer not exceeding x and some $J > 1$). The data modulated I- and Q-channel signature waveforms are defined by

$$c^{(k)}_{A,\langle m\rangle}(t) = \left[\sum_{n=0}^{N_f-1}\sum_{g=0}^{G-1} b^{(k)}_{A,\langle m\rangle}(g;n)\, p_{T_w}(t - gT_w - nT)\right] c_k(t) \tag{7}$$

for $A = I, Q$. Here, the modulating sequences $\{b^{(k)}_{I,\langle m\rangle}(g;n)\}$ and $\{b^{(k)}_{Q,\langle m\rangle}(g;n)\}$ are designed as multidimensional signals both in time and code spaces to provide multiple data rates.

The proposed multidimensional W-CDMA signaling can be modified in many ways, depending on how to construct the modulating sequences, and in turn affects the receiver structure at the base station. To maintain orthogonality among parallel transmissions, these sequences are allowed to be changed over each Walsh symbol in time space. Also, to keep receiver complexity manageable, they need to remain unchanged over more than one parallel transmission in code space. By observing these facts, we may propose one possible realization as follows: 1) the I-channel modulating sequence $\{b^{(k)}_{I,\langle m\rangle}(g;n) \,|\, g = 0, \ldots, G-1\}$ is determined in a certain manner from a set of G orthogonal codes $\{\mathbf{h}_i \,|\, i = 0, \ldots, G-1\}$ where $\mathbf{h}_i$ denotes the ith row vector of H_G; 2) such mapping is arranged for any subset $\{\mathbf{h}_i \,|\, i = 0, \ldots, L-1\}$ with $L = 2^l \leq G$ and an integer l (signaling order) ≥ 1; and 3) repeat 1) and 2) for the Q-channel modulating sequence $\{b^{(k)}_{Q,\langle m\rangle}(g;n) \,|\, g = 0, \ldots, G-1\}$. Here, each mapping is performed whenever the nth data symbol and $\langle m\rangle$th ($\langle m\rangle = \lfloor m/J \rfloor$) group of $J > 1$ parallel transmissions are ready for the I- and Q-channel, ranging $0 \leq n \leq N_f - 1$ and $0 \leq \langle m\rangle \leq M/J - 1$. This implies that the data rate can be increased to a maximum $[M + (M/J)\log_2 G]$ bits per symbol per channel subject to the constraints $G = T/T_w$ and $J > 1$ as key parameters (see Table I) in multidimensional signaling.

Here, we note that the multicode scheme is equivalent to the multidimensional signaling with $L = 1$ ($l = 0$), namely, $b^{(k)}_{I,\langle m\rangle}(g;n) = b^{(k)}_{Q,\langle m\rangle}(g;n) = 1$ for all $g = 0, \ldots, G-1$. Then, multidimensional signaling introduces additional L-ary ($1 < L \leq G$) orthogonal modulation for which symbol-by-symbol detection is required at the receiver. Thus, multidimensional signaling increases the data rate at the cost of receiver complexity. It is shown [14] that the symbol-error performance can be improved further even with increased rate, compared to the multicode scheme. Also, given the maximum rate above, a multicode scheme needs $[M + (M/J)\log_2 G]$ parallel (code) channels while multidimensional signaling requires only M, resulting in far reduced envelope variations.

Following the above design procedure, the resulting kth user's signal has the expression

$$\tilde{s}_k(t) = \sqrt{P}\left[\sum_{m=0}^{M-1}\sum_{n=0}^{N_f-1}\sum_{g=0}^{G-1}\Big[d^{(k)}_{I,m}(n) b^{(k)}_{I,\langle m\rangle}(g;n) \cdot p_{T_w}(t - gT_w - nT) + j d^{(k)}_{Q,m}(n) b^{(k)}_{Q,\langle m\rangle}(g;n) \cdot p_{T_w}(t - gT_w - nT)\Big] w_m(t)\right] c_k(t) \tag{8}$$

which is referred to as the *multidimensional W-CDMA signaling* that is illustrated in Fig. 1(b). Here, we are concerned with a

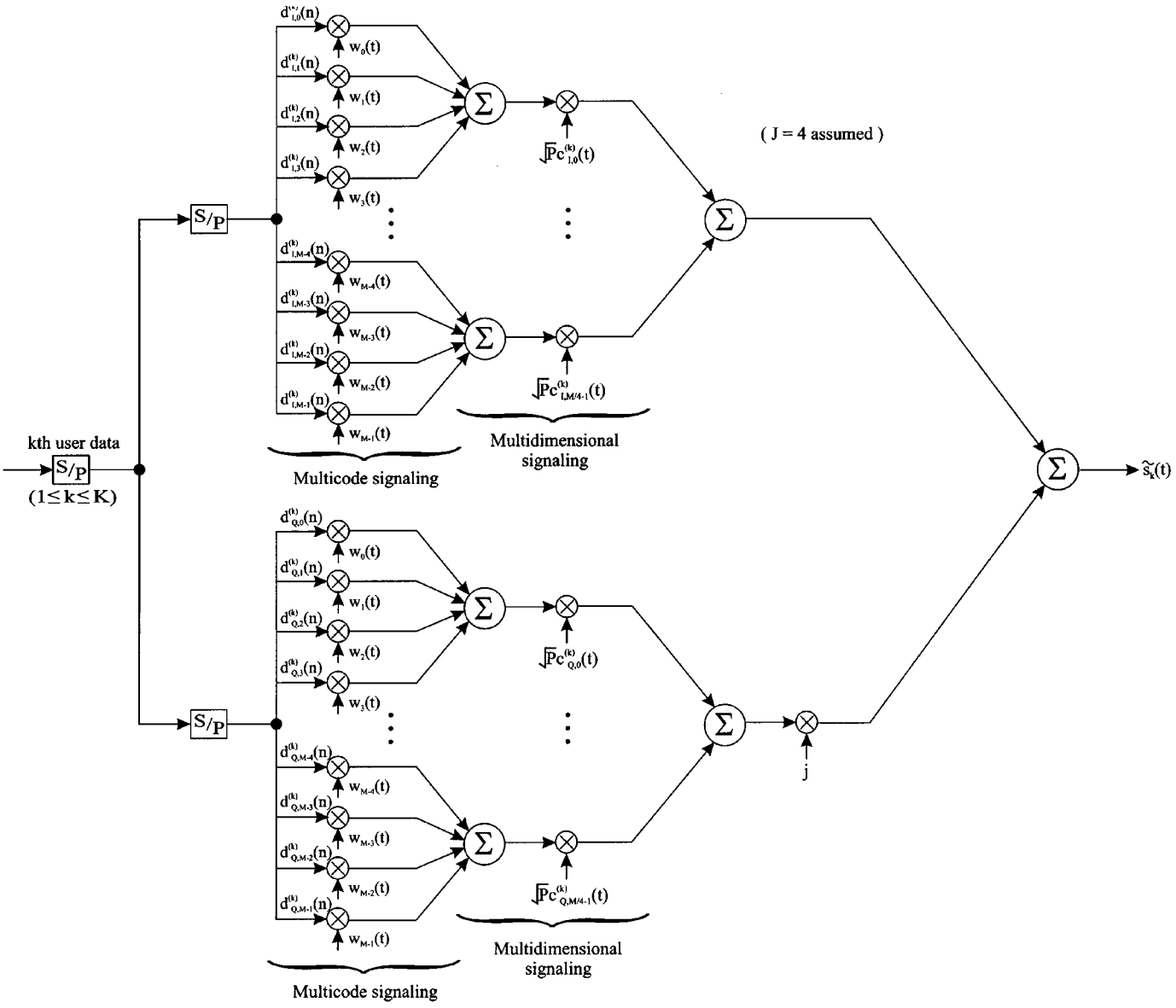

(b)

Fig. 1. *(Continued.)*Uplink W-CDMA system by the kth user's multidimensional signaling based on I- and Q-channel modulating sequences. (b) Multidimensional W-CDMA signaling.

CDMA-based cellular system and are considering a single cell with K (high-rate) users and a centered base station. By despreading an addressing portion of each user, his own transmission can be extracted in the presence of other user interferences, and then applying orthogonality in time and code spaces recovers an original data from symbol to symbol.

III. Signaling for Transmit Diversity and Gain

For the uplink W-CDMA channel of interest, the remote units have somewhat limited hardware complexity so that it is desirable to employ two antennas offering a simple two-branch transmit diversity. In connection with multidimensional signaling in time and code spaces, this diversity technique will benefit spatial separation between the two signals from each antenna. Hence, by using diversity combining at the base station, the uplink SIR can be further stabilized to provide additional gain when higher data rates are required, e.g., wireless multimedia services.

Regarding selection of transmit diversity scheme, the closed-loop techniques such as transmit adaptive arrays [7] and selective transmit diversity [8] may not be appropriate since there exist (inherent) channel estimation errors to which multidimensional signaling is sensitive because of the high-order modulation. Instead, the orthogonal transmit diversity (OTD) shown in [7, Fig. 2(a)] can be adopted as a simple means for providing the diversity gain of order 2. In reality, it is hard to obtain the diversity gain due to the small antenna separation in remote units. For this reason, the hybrid scheme[4] of OTD combined with delay diversity is considered to have uncorrelated received signals from the two antennas.

[4]If fairly uncorrelated antenna elements can be realized [15], then OTD only is used, but the analysis here still holds even with no delay, i.e., $D = 0$.

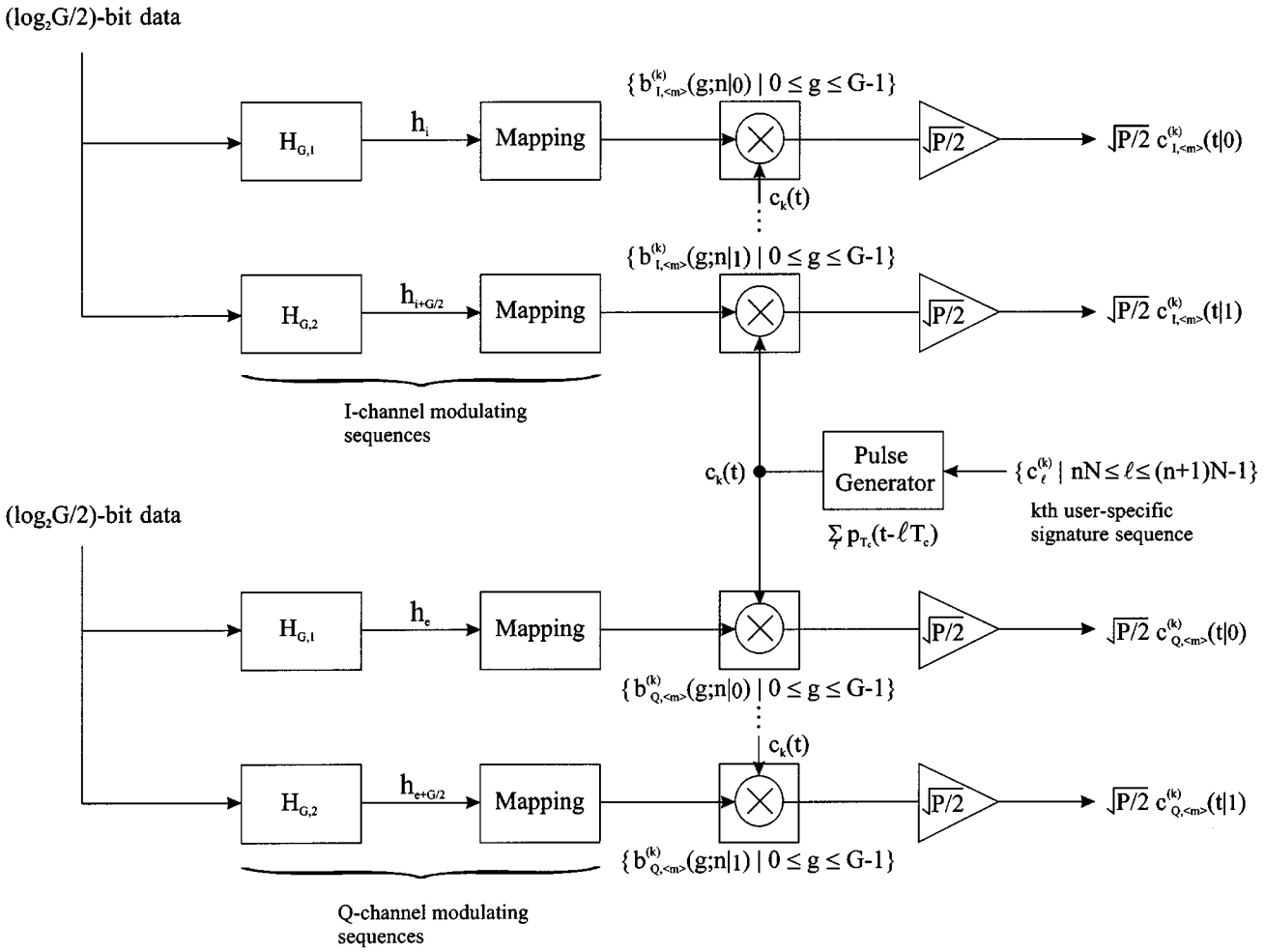

Fig. 2. Generation of data-modulated I- and Q-channel signature waveforms for two-branch transmit diversity.

The proposed multidimensional W-CDMA signaling is slightly changed to offer the transmit diversity of order 2 as follows: 1) the orthogonal matrix H_G is partitioned into two submatrices, namely, $H_G = [H_{G,1}^T \,|\, H_{G,2}^T]^T$ where $H_{G,1} = [\mathbf{h}_0^T, \ldots, \mathbf{h}_{G/2-1}^T]^T$ and $H_{G,2} = [\mathbf{h}_{G/2}^T, \ldots, \mathbf{h}_{G-1}^T]^T$ for T denoting the transpose and 2) each mapping of I- and Q-channel modulating sequences is arranged for any subset of $H_{G,1}$ and $H_{G,2}$ with the same size $L = 2^l \le G/2$ and an integer l. As shown in Fig. 2, such a mapping rule will generate

$$\left\{b_{I,\langle m\rangle}^{(k)}(g;n\,|\,q)\,|\,g=0,\ldots,G-1\right\} \to \mathbf{h}_{i+qG/2} \quad (9)$$

$$\left\{b_{Q,\langle m\rangle}^{(k)}(g;n\,|\,q)\,|\,g=0,\ldots,G-1\right\} \to \mathbf{h}_{e+qG/2} \quad (10)$$

for $0 \le i,e \le L-1$ and an index $q = 0,1$ indicating the $(q+1)$th transmit antenna.

Since each mapping is repeated for the two transmit antennas, the data rate will be sacrificed at the cost of diversity[5] that results in a maximum $[M + (M/J)\log_2(G/2)]$ bits per symbol per channel as a function of G and $J > 1$. Compared to the signaling in (8), we may have a loss in data rate as much as M/J, where the resulting kth user's signal for the $(q+1)$th transmit antenna is given by

$$\tilde{s}_k(t\,|\,q) = \sqrt{\frac{P}{2}}\left[\sum_{m=0}^{M-1}\sum_{n=0}^{N_f-1}\sum_{g=0}^{G-1}\left[d_{I,m}^{(k)}(n)b_{I,\langle m\rangle}^{(k)}(g;n\,|\,q)\cdot p_{T_w}(t-gT_w-nT) + jd_{Q,m}^{(k)}(n)b_{Q,\langle m\rangle}^{(k)}(g;n\,|\,q)\cdot p_{T_w}(t-gT_w-nT)\right]w_m(t)\right]c_k(t). \quad (11)$$

Here, $\tilde{s}_k(t\,|\,q)$ can be illustrated in Fig. 1 by replacing $\sqrt{P}c_{A,\langle m\rangle}^{(k)}(t)$ with $\sqrt{P/2}c_{A,\langle m\rangle}^{(k)}(t\,|\,q)$ $(A = I,Q)$ in Fig. 2. Note that the transmit power P per (code) channel is equally divided, and $P/2$ is assigned to each antenna.

Now the kth user's signal $\tilde{s}_k(t) = \tilde{s}_k(t\,|\,0) + \tilde{s}_k(t-D\,|\,1)$ will be transmitted under CDMA-based cellular system, where the delay $D \ge T + (\text{delay spread})$ is needed to achieve uncorrelated signals and the maximum diversity gain at the receiver [3], [4]. Here, the difference between propagation delays due to the delay is ignored[6] so that the signals from each antenna are assumed to arrive at the receiver after a channel delay

[5]We may circumvent this by incorporating the other OTD scheme shown in Fig. 2(b) of [7], but the diversity gain of order 2 is not achieved.

[6]We may have some offsets in those delays, but their effects would not change fading statistics because of uniform channel delay assumptions.

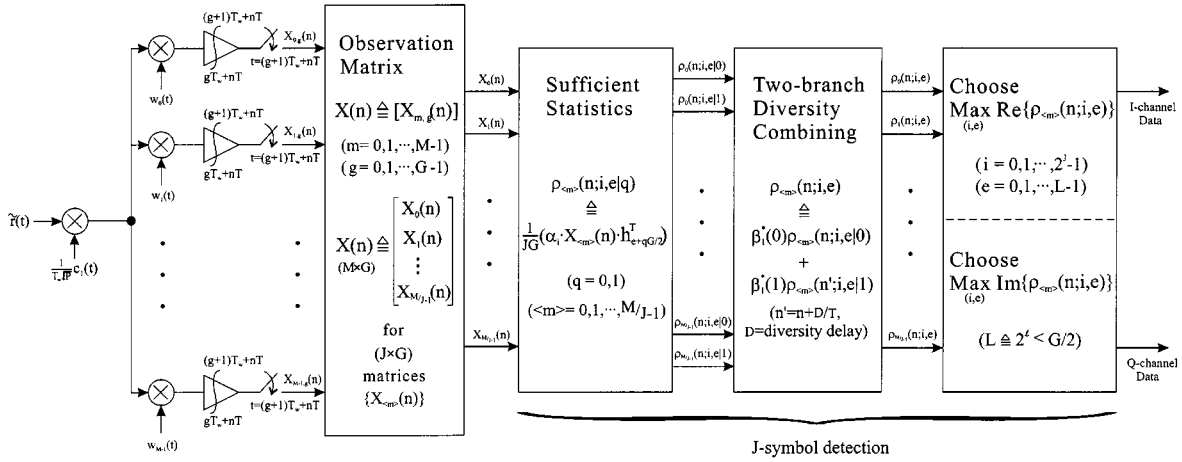

Fig. 3. Receiver structure with two-branch diversity combining and J-symbol detection for the first user.

TABLE I
PARAMETERS OF IMPORTANCE FOR MULTIDIMENSIONAL SIGNALING

Parameter	Definition / Explanations
N_f	number of symbols (bauds) per frame
T	symbol (baud) time
T_w	walsh symbol time
T_c	walsh chip time
G	degree of freedom in time space, where $G \triangleq T/T_w$
M	degree of freedom in code space, where $M \triangleq T_w/T_c$
N	total degree of freedom in signal space, where $N \triangleq GM$ or spreading factor per symbol
L	$L = 2^l \le G(G/2)$ without(with) transmit diversity where l is the order of multidimensional signaling
J	number of parallel (code) channels per L-ary orthogonal modulation

of $\tau_k + qD, k = 1,\ldots,K$ and $q = 0,1$, because of asynchronous transmission and delay diversity, the delays $\{\tau_k\}$ uniformly distributed over $[0,T)$. Then, a composite signal is delayed by $\{\tau_k + qD\}$ and weighted by the complex fade coefficients $\{\beta_k(q)\}$ $(q = 0,1)$ modeled as zero-mean complex-valued Gaussian, which is observed by the receiver as

$$\tilde{r}(t) = \sum_{k=1}^{K} [\beta_k(0)\tilde{s}_k(t-\tau_k\,|\,0) + \beta_k(1)\tilde{s}_k(t-\tau_k-D\,|\,1)]. \tag{12}$$

It should be noted that the delay $D = lT$ (some integer l) is inserted and the user-specific signature sequence $c_k(t+qD)$ is used instead of $c_k(t)$ in (11), because one sequence generator is required for each user and channel orthogonalization is still valid for the two antennas.

After despreading, the first user's received signal energy is resolved into code and time spaces using the orthogonality like

$$X_{m,g}(n) = \frac{1}{T_w\sqrt{P}} \int_{gT_w+nT}^{(g+1)T_w+nT} \tilde{r}(t)c_1(t)w_m(t)\,dt \tag{13}$$

where $m = 0,\ldots,M-1; g = 0,\ldots,G-1$ and τ_1 is simply assumed to be zero. Let us define a matrix $X_{\langle m\rangle}(n)$ with elements $\{X_{m',g}(n)\,|\,m' = \langle m\rangle J,\ldots,\langle m\rangle J+J-1; g = 0,\ldots,G-1\}$, and then the resolved energies are collected by forming sufficient statistics such as

$$\rho_{\langle m\rangle}(n;i,e\,|\,q) = \frac{1}{JG}\left(\alpha_i \cdot X_{\langle m\rangle}(n)\cdot \mathbf{h}_{e+qG/2}^T\right) \tag{14}$$

in which $i = 0,\ldots,2^J-1; e = 0,\ldots,L-1; q = 1,0$ and α_i is a J-tuple row vector with elements ± 1. Finally, two-branch diversity combining yields

$$\rho_{\langle m\rangle}(n;i,e) = \beta_1^*(0)\rho_{\langle m\rangle}(n;i,e\,|\,0) + \beta_1^*(1)\rho_{\langle m\rangle}(n+D/T;i,e\,|\,1) \tag{15}$$

for the complex conjugate $*$, and then $\mathrm{Re}\{\cdot\}$ and $\mathrm{Im}\{\cdot\}$ produce the I- and Q-channel decision variables, respectively. The receiver structure being considered is shown in Fig. 3.

To gain insight on the transmit diversity, we investigate the probability distribution function (p.d.f.) of $\mathrm{Re}\{\rho_{\langle m\rangle}(n;i,e)\}$ in Appendix A which is asymptotically Gaussian as K increases. It follows that the p.d.f. $f(y)$ of $Y \triangleq Z - \mathbf{E}\{Z\}$; an expectation $\mathbf{E}$; $Z \triangleq \mathrm{Re}\{\rho_{\langle m\rangle}(n;i,e)\}$; can be formulated as

$$f(y) = \frac{1}{\sigma_I}\left[\phi\left(\frac{y}{\sigma_I}\right) + \frac{a_4}{(K-1)}\phi^{(4)}\left(\frac{y}{\sigma_I}\right) + \frac{a_6}{(K-1)^2}\phi^{(6)}\left(\frac{y}{\sigma_I}\right) + \cdots\right] \tag{16}$$

where $\sigma_I^2 = \mathbf{E}\{Y^2\}$, the Gaussian function $\phi(x) = 1/\sqrt{2\pi}\exp(-x^2/2)$, and its nth derivative $\phi^{(n)}(x)$. Here, the coefficient a_n (an even integer $n \ge 4$) can be determined by the formula [16]

$$a_n = \frac{(-1)^n}{n!}\int_{-\infty}^{\infty} f_k(y)H_n(y)\,dy \tag{17}$$

where $f_k(y)$ denotes the p.d.f. of $Y_k = Z_k/\sigma_{I,k}; \sigma_{I,k}^2 = \mathbf{E}\{Z_k^2\}$ $(k \ge 2)$, and Z_k is the kth user term in Z, namely, $Z = \sum_{k=1}^{K} Z_k$. Also, the Hermite polynomials $\{H_n(y)\}$ are recursively calculated by $H_{n+1}(y) = yH_n(y) - nH_{n-1}(y)$ with initial value $H_0(y) = 1$.

For simplicity, if K is sufficiently large, then a_4 in $f(y)$ may be a dominant factor to see how far it diverges from asymptotic

Gaussian. In Appendix A, we evaluate the coefficient a_4 for the two cases, i.e.,

$$a_4 \cong \begin{cases} \Delta/16 - 1/12, & \text{with transmit diversity,} \\ (\Delta - 1)/8, & \text{without transmit diversity} \end{cases} \tag{18}$$

where

$$\Delta = \left[\frac{\mathbf{E}\{\bar{\eta}^4(\delta)\}}{\mathbf{E}^2\{\bar{\eta}^2(\delta)\}} + \frac{\mathbf{E}\{\bar{\eta}^2(\delta)\bar{\eta}^2(T_c - \delta)\}}{\mathbf{E}^2\{\bar{\eta}^2(\delta)\}} \right] \tag{19}$$

for $\bar{\eta}(\delta) = 1/T_c \int_0^\delta p_{T_c}(t) p_{T_c}(t + T_c - \delta)\, dt$, δ uniformly distributed over $[0, T_c)$. Since a unit-magnitude rectangular pulse $p_{T_c}(t)$ gives $\Delta = 2.1$, $a_4 \cong 0.0479, 0.1375$ (ratio $\cong 2.87$) for the two schemes. This implies that statistics in Y become more Gaussian when the transmit diversity is used, which benefits diversity gain [17].

IV. The Average Probability of Symbol Error

In fact, the effect of nonlinear distortion exists in the uplink of a W-CDMA channel which results from multilevel amplitude characteristics because of multicode signaling and using a cost-effective nonlinear amplifier. To allow possible theoretical evaluation, analysis here is confined to the multidimensional signaling with a constant envelope so that the input symbol α_i becomes a $J(4)$-tuple row vector whose element '1' exists as many as an odd number, i.e., 1 or 3 [14]. When $M = 16$, a precoding method can be introduced to maintain the constant envelope property as shown in [14]. For the other cases such as $M \neq 2^{2n}$ $(n \geq 1)$, it is required that simulation be performed to properly integrate the above nonlinear effect.

Let us simply denote $\rho_r(i,e) = \mathrm{Re}\{\rho_{\langle m \rangle}(n;i,e)\}$, and then the decision variable $\rho_r(i,e)$ is formed into

$$\rho_r(i,e) = D_r(i,e) + \sum_{k=1}^{K} I_r^{(k)}(i,e) + N_r(i,e) \tag{20}$$

where $D_r(i,e)$ is the desired signal, $I_r^{(k)}(i,e)$ is the kth user interference term, and $N_r(i,e)$ is the filtered background noise. Here, the uplink channel is generalized to include multipath delayed terms with either equal or unequal average path powers,[7] in which (12) is rewritten as

$$\tilde{r}(t) = \sum_{k=1}^{K} \sum_{v=1}^{V} [\beta_{k,v}(0)\tilde{s}_k(t - \tau_{k,v} \,|\, 0) + \beta_{k,v}(1)\tilde{s}_k(t - \tau_{k,v} - D \,|\, 1)] + \tilde{n}(t) \tag{21}$$

with V paths and a complex-valued Gaussian noise $\tilde{n}(t)$ of p.s.d. $N_o/2$. We assume that $\{\beta_{k,v}(q)\}$ and $\{\tau_{k,v}\}$ indicate the sets of fade coefficients and delays of the kth user and vth path, mutually independent, from the $(q+1)$th transmit antenna. Then, the diversity combining in (15) can be expressed by

$$\rho_{\langle m \rangle}(n;i,e) = \sum_{v=1}^{V} \left[\beta_{1,v}^*(0)\rho_{\langle m \rangle}^{(v)}(n;i,e \,|\, 0) + \beta_{1,v}^*(1)\rho_{\langle m \rangle}^{(v)}(n + D/T;i,e \,|\, 1) \right] \tag{22}$$

[7]Due to offsets in propagation delays, the individual path gains averaged over a fading may be changed with delayed versions of a signal, but the second-order effects are ignored here for analysis.

in which $(q = 0, 1)$

$$\rho_{\langle m \rangle}^{(v)}(n;i,e \,|\, q) = \frac{1}{JG} \left(\alpha_i \cdot X_{\langle m \rangle}(n;v) \cdot \mathbf{h}_{e+qG/2}^T \right) \tag{23}$$

and the matrix $X_{\langle m \rangle}(n;v)$ has the element

$$X_{m',g}(n;v) = \frac{1}{T_w \sqrt{P}} \int_{gT_w + nT + \tau_{1,v}}^{(g+1)T_w + nT + \tau_{1,v}} \tilde{r}(t) c_1(t - \tau_{1,v}) \cdot w_{m'}(t - \tau_{1,v})\, dt \tag{24}$$

for $m' = \langle m \rangle J, \ldots, \langle m \rangle J + J - 1$.

In Appendix B, statistics on $D_r(i,e), I_r^{(k)}(i,e)$ and $N_r(i,e)$ are characterized in detail, and it turns out that $\{\rho_r(i,e)\}$ forms a set of statistically biorthogonal random variables when α_i belongs to the subset $\{\alpha_l \,|\, l = 1, 2, 4, 7, 8, 11, 13, 14\}$. Then, the average probability of symbol error, $P(\epsilon)$, is formulated as

$$P(\epsilon) = \frac{1}{8L} \sum_{(i,e)} P(\epsilon \,|\, \alpha_i, \mathbf{h}_{e+qG/2}) \tag{25}$$

for which the input symbol $\{d_{I,m'}^{(1)}(n)\} \rightarrow \alpha_i$ (n fixed) and the modulating sequence $\{b_{I,\langle m \rangle}^{(1)}(g; n \,|\, q)\} \rightarrow \mathbf{h}_{e+qG/2}$ were sent. Due to the biorthogonality, i.e., $\rho_r(i',e') = -\rho_r(15 - i', e')$ $(i' = 1, 2, 4, 7, 8, 11, 13, 14; e' = 0, \ldots, L-1)$ and invoking the Gaussian assumption on $\{I_r^{(k)}\}$, it can be simplified to [18]

$$\begin{aligned} &P(\epsilon \,|\, \alpha_i, \mathbf{h}_{e+qG/2}) \\ &\quad = 1 - \Pr\left[\bigcap_{(i',e') \neq (i,e)} \rho_r(i';e') < \rho_r(i;e) \,\middle|\, \alpha_i, \mathbf{h}_{e+qG/2} \right] \\ &\quad = 1 - \int_0^\infty \Pr^{4L-1}[|\rho_r(i',e')| < \rho_r(i,e) = \zeta > 0 \,|\, \alpha_i, \\ &\qquad \mathbf{h}_{e+qG/2}] f(\zeta \,|\, \alpha_i, \mathbf{h}_{e+qG/2})\, d\zeta \end{aligned} \tag{26}$$

for $(i',e') \neq (i,e)$ or $(15 - i, e)$, where $f(\zeta \,|\, \alpha_i, \mathbf{h}_{e+qG/2})$ denotes the p.d.f. of $\rho_r(i,e)$. After a few manipulations, it can be placed into the compact form

$$P(\epsilon \,|\, \alpha_i, \mathbf{h}_{e+qG/2}) = 1 - \int_0^\infty [1 - 2Q(\xi)]^{4L-1} \cdot \mathbf{E}_\gamma\{\phi(\xi - \sqrt{\gamma})\}\, d\xi \tag{27}$$

in which $Q(\xi) = \int_\xi^\infty \phi(x)\, dx$ and γ represents the effective SNR in Appendix B as

$$\gamma = \frac{1}{2} \sum_{v=1}^{V} [|\beta_{1,v}(0)|^2 + |\beta_{1,v}(1)|^2] \Bigg/ \left[(8E/N_o)^{-1} + (M/4N)\mathbf{E}\{\bar{\eta}^2(\delta)\} \cdot \left(K_* \sum_{v=1}^{V} \mathbf{E}\{|\beta_{k,v}(0)|^2 + |\beta_{k,v}(1)|^2\} \right) \right] \tag{28}$$

with $K_* = (K-1) + (V-1)/V$.

Based on $\{|\beta_{k,v}(q)|\}$ having equal or unequal average path powers, the expectation in (27) may be evaluated as follows. First, we assume that $\mathbf{E}\{|\beta_{k,v}(q)|^2\} = \sigma_\beta^2$ for all k, v, q, in which $\Psi \triangleq \sum_{v=1}^{V}[|\beta_{1,v}(0)|^2 + |\beta_{1,v}(1)|^2]$ has the distribution [16]

$$f(\psi) = \frac{1}{\left(\sigma_\beta^2\right)^{2V}(2V-1)!}\psi^{2V-1}\exp\left(-\frac{\psi}{\sigma_\beta^2}\right). \quad (29)$$

By taking an expectation with respect to Ψ, it follows that

$$\begin{aligned}\mathbf{E}_\gamma\{\phi(\xi-\sqrt{\gamma})\} &= \frac{(4V-1)!}{(2)^{4V-1}(2V-1)!}\frac{\exp(-\xi^2/2)}{(1+\gamma_*)^{2V}} \\ &\cdot\left[\frac{1}{\sqrt{2}\Gamma(2V+1/2)}{}_1F_1\left(2V,\frac{1}{2},\frac{\xi^2}{2(1+\gamma_*^{-1})}\right)\right. \\ &\left.+\frac{\xi}{\Gamma(2V)\sqrt{1+\gamma_*^{-1}}}{}_1F_1\left(2V+\frac{1}{2},\frac{3}{2},\frac{\xi^2}{2(1+\gamma_*^{-1})}\right)\right] \quad (30)\end{aligned}$$

where the per-path, per-(code) channel effective SNR is defined by

$$\gamma_* = \left[\left(2\sigma_\beta^2 E/N_o\right)^{-1} + (2M/N)(K_*V)\mathbf{E}\{\bar{\eta}^2(\delta)\}\right]^{-1} \quad (31)$$

and $\Gamma(\cdot)$ is the gamma function and ${}_1F_1(\cdot,\cdot,\cdot)$ the confluent hypergeometric function [19].

Next, under the unequal average path powers, assume that $\mathbf{E}\{|\beta_{k,v}(q)|^2\} \neq \mathbf{E}\{|\beta_{k,v'}(q)|^2\}$ $(v \neq v')$ and $\mathbf{E}\{|\beta_{k,v}(q)|^2\} = \sigma_\beta^2(v)$ for all k, q. In Appendix C, the p.d.f. of Ψ is derived as

$$\begin{aligned}f(\psi) &= \sum_{v=1}^{V}\frac{\pi_v^2}{\sigma_\beta^4(v)}\psi\exp\left(-\frac{\psi}{\sigma_\beta^2(v)}\right) \\ &+\sum_{v=1}^{V}\sum_{\substack{v'=1\\v'\neq v}}^{V}\frac{\pi_v\pi_{v'}}{\sigma_\beta^2(v)-\sigma_\beta^2(v')} \\ &\cdot\left[\exp\left(-\frac{\psi}{\sigma_\beta^2(v)}\right)-\exp\left(-\frac{\psi}{\sigma_\beta^2(v')}\right)\right] \quad (32)\end{aligned}$$

where $\pi_v = \prod_{\substack{v'=1\\v'\neq v}}^{V}\sigma_\beta^2(v)/[\sigma_\beta^2(v)-\sigma_\beta^2(v')]$. Similarly, taking the expectation in (27) yields

$$\begin{aligned}\mathbf{E}_\gamma\{\phi(\xi-\sqrt{\gamma})\} &= \sum_{v=1}^{V}\pi_v^2\left\{\left[1+\frac{\xi^2}{2[1+(\gamma_*\theta_v)^{-1}]}\right]\Phi_2(\xi,\gamma_*\theta_v)\right. \\ &\left.+\frac{1}{2}\left[3+\frac{\xi^2}{[1+(\gamma_*\theta_v)^{-1}]}\right]\Omega_2(\xi,\gamma_*\theta_v)\right\} \\ &+\sum_{v=1}^{V}\sum_{\substack{v'=1\\v'\neq v}}^{V}\frac{\pi_v\pi_{v'}}{(\theta_v-\theta_{v'})}[\theta_v\Phi_1(\xi,\gamma_*\theta_v)-\theta_{v'}\Phi_1(\xi,\gamma_*\theta_{v'}) \\ &+\theta_v\Omega_1(\xi,\gamma_*\theta_v)-\theta_{v'}\Omega_1(\xi,\gamma_*\theta_{v'})] \quad (33)\end{aligned}$$

in which the per-path, per-(code) channel effective SNR is defined by

$$\gamma_* = \left[\left(2\sigma_\beta^2(1)E/N_o\right)^{-1} + (2M/N)\left(K_*\sum_{v=1}^{V}\theta_v\right)\mathbf{E}\{\bar{\eta}^2(\delta)\}\right]^{-1} \quad (34)$$

with $\theta_v = \sigma_\beta^2(v)/\sigma_\beta^2(1)$, and

$$\begin{aligned}\Phi_n(\xi,u) &= \frac{1}{\sqrt{2\pi}(1+u)^n}\exp\left(-\frac{\xi^2}{2}\right) \\ \Omega_n(\xi,u) &= \frac{\xi}{\sqrt{1+u^{-1}}(1+u)^n}\exp\left(-\frac{\xi^2}{2(1+u)}\right) \\ &\cdot\left[1-Q\left(\frac{\xi}{\sqrt{1+u^{-1}}}\right)\right].\end{aligned}$$

Finally, to compare the two schemes, i.e., with/without transmit diversity, we consider a single-antenna transmission with transmit power P per (code) channel instead of $P/2$, assuming the same signaling and data rate. By reflecting only the case $q = 0$, it is easy to show that $P(\epsilon)$ is given by (25)–(27) with such modifications as

$$\gamma = \frac{\sum_{v=1}^{V}|\beta_{1,v}(0)|^2}{[(8E/N_o)^{-1}+\sigma_I^2]} \quad (35)$$

$$\sigma_I^2 \cong (M/2N)\mathbf{E}\{\bar{\eta}^2(\delta)\}\left[K_*\sum_{v=1}^{V}\mathbf{E}\{|\beta_{k,v}(0)|^2\}\right]. \quad (36)$$

Now the p.d.f.s of $\Psi \triangleq \sum_{v=1}^{V}|\beta_{1,v}(0)|^2$, for equal and unequal average path powers, reduce to (29) with $2V$ replaced by V [16], and

$$f(\psi) = \sum_{v=1}^{V}\frac{\pi_v}{\sigma_\beta^2(v)}\exp\left(-\frac{\psi}{\sigma_\beta^2(v)}\right) \quad (37)$$

[13], respectively.

If we take an average with respect to Ψ, then $\mathbf{E}_\gamma\{\phi(\xi-\sqrt{\gamma})\}$ in the former case is given by (30) with $2V$ and γ_* replaced by V and $2\gamma_*$, respectively. Similarly, it is evaluated that for the latter case

$$\mathbf{E}_\gamma\{\phi(\xi-\sqrt{\gamma})\} = \sum_{v=1}^{V}\pi_v[\Phi_1(\xi,2\gamma_*\theta_v)+\Omega_1(\xi,2\gamma_*\theta_v)]. \quad (38)$$

V. Results

From the theoretical approach on diversity gain in Section III, we observed that two-branch transmit diversity helps the other-user interference to be more Gaussian, and also become asymptotically Gaussian as K increases. Along with the facts, we will demonstrate that the multidimensional signals with transmit diversity (TD) provide substantial gain over those without transmit diversity, and furthermore the nonmulticode scheme using a single spreading code. To avoid worse nonlinear distortions in uplink, we introduce a constant amplitude coding [20], [14] to the multidimensional W-CDMA signaling,

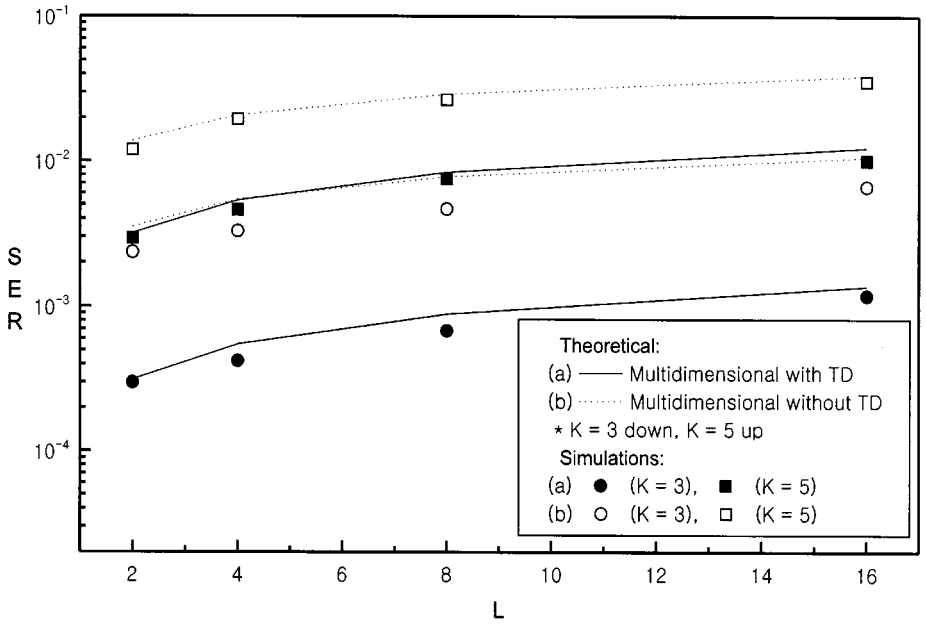

Fig. 4. SER $P(\epsilon)$ versus $L = 2^l, l$ (signaling order) $= 1, 2, 3, 4$ when $K = 3, 5, M = 4$ $(G/2 = 16), N = 128$ and $E/N_o = \infty$.

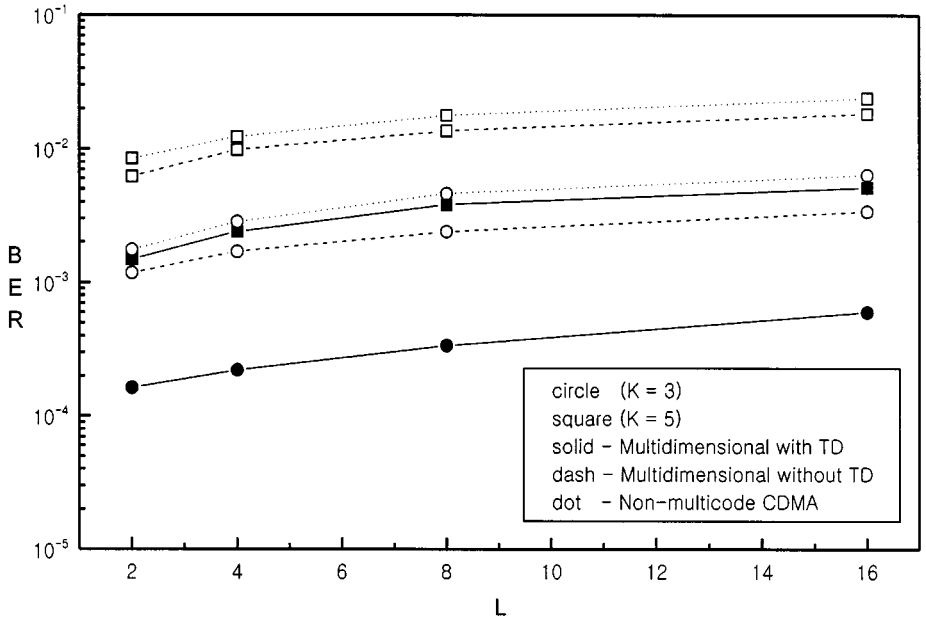

Fig. 5. BER versus $L = 2^l, l$ (signaling order) $= 1, 2, 3, 4$ when $K = 3, 5, M = 4$ $(G/2 = 16), N = 128$ and $E/N_o = \infty$, assuming $N = 128$ $(L = 2), N = 130$ $(L = 4)$, and $N = 126$ $(L = 8, 16)$ for the nonmulticode scheme.

where $\alpha_i \in \{\alpha_l \,|\, l = 1,2,4,7,8,11,13,14\}$ in connection with $J(4)$-symbol detection. For simulations, the signature waveform $c^{(k)}_{A,\langle m\rangle}(t \,|\, q)$ in Fig. 2 $(A = I, Q, q = 0, 1)$ was generated by using the long PN sequence with $g(x) = x^{42}+x^{35}+x^{33}+x^{31}+x^{27}+x^{26}+x^{25}+x^{22}+x^{21}+x^{19}+x^{18}+x^{17}+x^{16}+x^{10}+x^7+x^6+x^5+x^3+x^2+x+1, g(x)$ generator polynomial where the user-specific sequences $\{c^{(k)}_l\}$ are obtained by shifting its initial phase.

First, the symbol-error rate (SER) $P(\epsilon)$ is evaluated as a function of L by which the order of multidimensional signaling is determined. L can be varied from 2, 4, 8 up to 16, which means that an additional 1–4 bits are sent per the multicode signaling with $J = 4$ in Fig. 1(b) for a given I- or Q-channel. Fig. 4 shows $P(\epsilon)$ for the two schemes when $K = 3, 5, M = 4\,(G/2 = 16), N = 128$ and $E/N_o = \infty$ are considered, assuming $V = 3$-path Rayleigh fading with equal average path power. We note that the transmit diversity provides approximately double the user capacity compared to that with no diversity, because the former is as robust as the latter in the presence of $K - 1 = 4$-user and $K - 1 = 2$-user interferences, respectively. As expected, $P(\epsilon)$ is slightly degraded when more additional data are sent, but the degradation may be within an acceptable range. It should be noted that the transmit diversity makes the interferences more Gaussian while the theoretical results based on Gaussian assumption diverge from the simulation results in the case of no diversity, especially for a small number of users, $K = 3$.

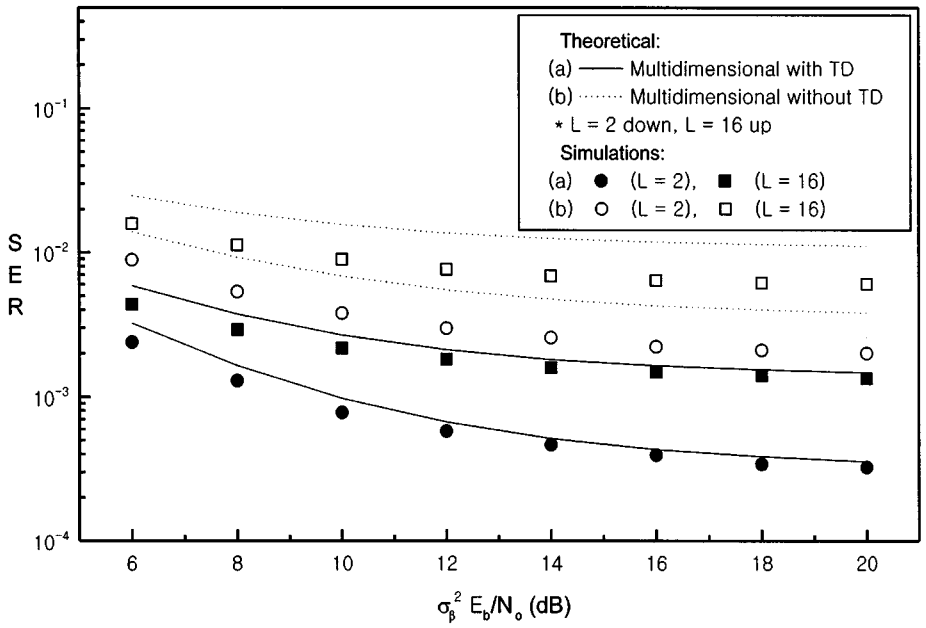

Fig. 6. SER $P(\epsilon)$ versus $\sigma_\beta^2 E_b/N_o$ when $K = 3, M = 4$ $(G/2 = 16), N = 128$ and $L = 2, 16$.

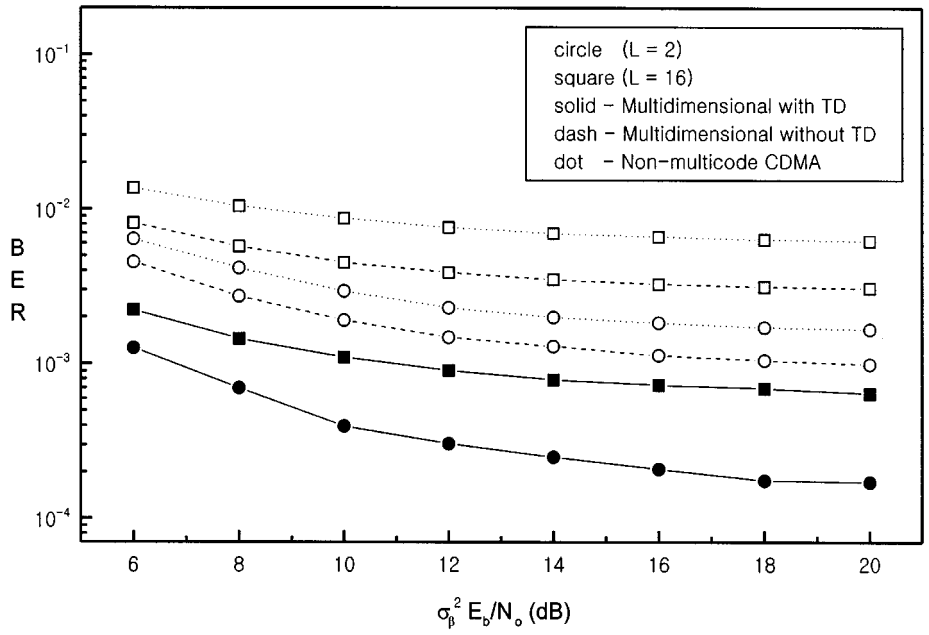

Fig. 7. BER versus $\sigma_\beta^2 E_b/N_o$ when $K = 3, M = 4$ $(G/2 = 16), N = 128$ and $L = 2, 16$, assuming $N = 128$ $(L = 2), N = 130$ $(L = 4)$, and $N = 126$ $(L = 8, 16)$ for the nonmulticode scheme.

In addition, the comparisons are extended to include the nonmulticode CDMA for which the BER was evaluated by performing simulations. Fig. 5 shows the BER curves for the above three schemes assuming the set of same parameters, except for the distinct spreading factors $N = 128\,(L = 2), N = 130\,(L = 4)$, and $N = 126\ (L = 8, 16)$ for the nonmulticode scheme, which give rise to an integer multiple chips per bit. Using the rate of $(3 + \log_2 L)$ bits per (I or Q) channel, the bit energy E_b is related to the signal energy per (code) channel as $E = E_b \cdot (3 + \log_2 L)/4$ for $M = 4$. The nonmulticode CDMA performs worst than others, that implies the benefit offered by the multidimensional signaling. Also, it is shown that the multidimensional signals with transmit diversity can increase the user capacity by a factor of two, compared to the variable spreading gain approach like nonmulticode CDMA.

To see the effect of background noise, the comparisons are made facing with both the other-user interferences and noise. Fig. 6 shows $P(\epsilon)$ versus $\sigma_\beta^2 E_b/N_o$, per-path bit SNR when $K = 3, M = 4$ $(G/2 = 16), N = 128$ and $L = 2, 16$ are considered. It is seen that the scheme with no diversity is less Gaussian, which causes a divergence of the curves obtained by the Gaussian approximation. Here, the degradation incurred by the noise is not as significant while the other-user interferences are a main factor to determine the user capacity. Fig. 7 compares the three schemes in terms of the BER versus $\sigma_\beta^2 E_b/N_o$, assuming the same N's in Fig. 5 for the nonmulticode scheme

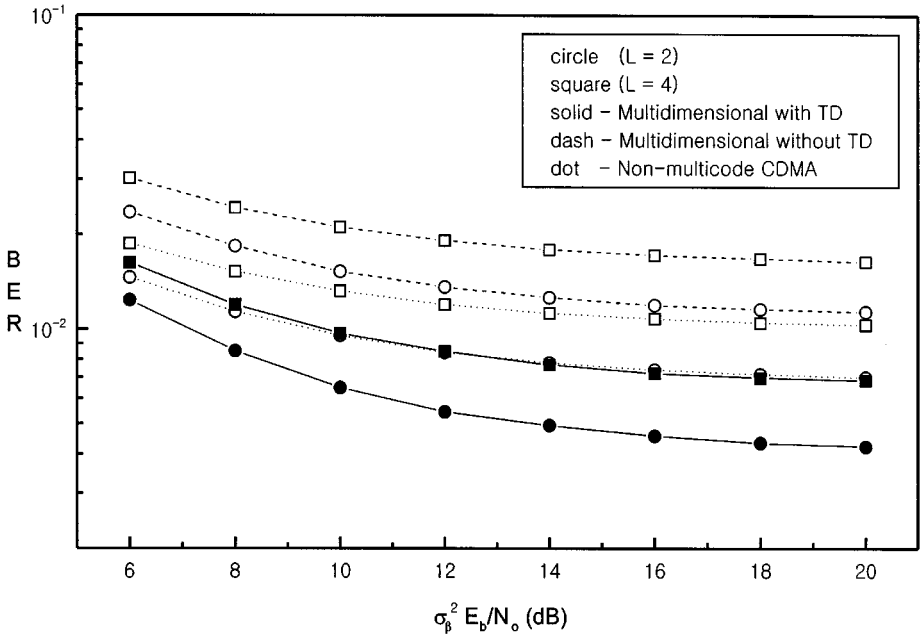

Fig. 8. BER versus $\sigma_\beta^2 E_b/N_o$ when $K = 2, M = 16\ (G/2 = 4), N = 128$ and $L = 2, 4$, assuming $N = 132\ (L = 2)$ and $N = 135\ (L = 4)$ for the nonmulticode scheme.

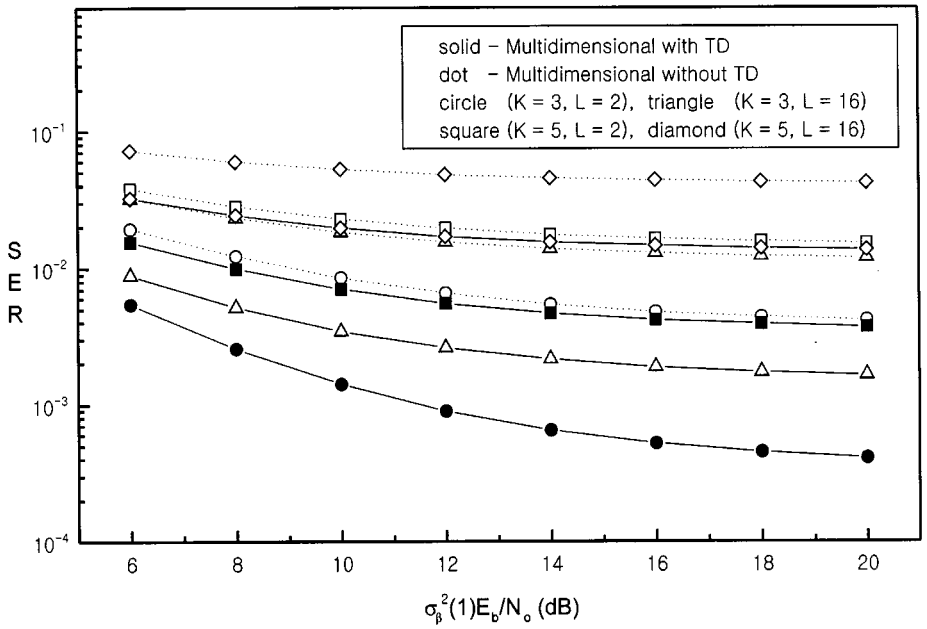

Fig. 9. SER $P(\epsilon)$ versus $\sigma_\beta^2(1)E_b/N_o$ when $K = 3, 5, M = 4\ (G/2 = 16), N = 128$ and $L = 2, 16$, assuming unequal average path powers with decay factor $\varepsilon = 0.3$.

and the same of set parameters above. A similar behavior of BER curves is observed so that the nonmulticode CDMA yields the worst performance for both $L = 2, 16$.

Next, to look at the effect of the number of (code) channels, M, we consider $M = 16$ which allows us to construct a constant envelope signal based on the procoding method in [14]. Here, $L = 2^l$ (l signaling order) is limited to $L = 2, 4$ due to $N = GM$ and $L \leq G/2$ when $N = 128$ and $M = 16$ are used. The additional data of 1 or 2 bits can be sent per the multicode signaling of $J = 4$, which produces an increase of 3 or 6 bits per $M = 16$-(code) channel compared to the constant amplitude coding in [20]. Thus, the signal energy E per (code) channel is given by $E = E_b \cdot 3(3 + \log_2 L)/16$, and hence we may have a loss in signal energy incurred by the precoding. In Fig. 8, the BER curves are shown versus $\sigma_\beta^2 E_b/N_o$ for the three schemes when $K = 2, M = 16\ (G/2 = 4)$ and $N = 128$ are considered, except that $N = 132\ (L = 2)$ and $N = 135\ (L = 4)$ are used to give an integer number of chips per bit for the nonmulticode scheme. We note that the multidimensional signals with transmit diversity yield the lowest BER, and also allow sending the additional data of 3 bits with $L = 4$ compared to the nonmulticode scheme with rate of 12 bits per $N = 132$ chips $(L = 2)$ per (I or Q) channel while performing comparably. But the multidimensional signals with no diversity

are severely degraded in part because of the loss in E by the precoding, and in part because of no diversity gain.

Finally, under unequal average path powers, $P(\epsilon)$ is plotted versus $\sigma_\beta^2(1)E_b/N_o$ in Fig. 9 for the two schemes when $K = 3, 5, M = 4$ $(G/2 = 16)$, $N = 128$ and $L = 2, 16$ are considered. Here, the parameter $\theta_v = \sigma_\beta^2(v)/\sigma_\beta^2(1) = \exp[-(v-1)\cdot \varepsilon]$ $(v = 1, 2, 3)$ is adopted for the decay factor $\varepsilon = 0.3$, which gives an exponentially decaying multipath profile. We find that the diversity gain can be achieved by a factor of two for both $L = 2, 16$, and also the scheme with diversity can increase the rate up to 7 bits per (I or Q) channel without deteriorating $P(\epsilon)$ compared to that with no diversity (rate of 4 bits per channel).

VI. Conclusion

A newly designed multidimensional W-CDMA signal has been applied to provide a diversity order of 2 in uplink transmission for two transmit antennas and one receive antenna. The signal is quite flexible in changing the rate depending on the incoming traffics because of the signal characteristics exploiting both the code and time spaces, and easily modified to allow spatial separation. Also, it has the characterisitcs of multicode signaling that gives rise to large envelope variations, but a multidimensional signal reduces the number of parallel channels to help minimize the envelope variations. Further, a precoding is adopted to produce a constant envelope signal while high and multiple data rates are offered at the same time.

A theoretical approach to diversity gain showed that the interferences can be made more Gaussian by the transmit diversity, offering additional gain. It was found that the use of transmit diversity results in approximately double the user capacity, because the signaling with diversity shows the capability of rejecting the interferences from double the users in the case of no diversity. In view of the BER, the nonmulticode scheme performed worst so that we can achieve a certain gain by the multidimensional signaling for $M = 4$-parallel (code) channels while the signaling with diversity provides a gain of order 2 in user capacity compared to the nonmulticode scheme. Even with $M = 16$-parallel (code) channels, the signaling with diversity can assure a gain of 25% increase in data rate over the nonmulticode scheme.

Appendix A
Evaluation of the Coefficient a_4 in (16)

To estimate the p.d.f. $f(y)$ in (16), the output (13) is first formulated as

$$X_{m,g}(n) = \frac{1}{2M}\sum_{l=0}^{M-1} c^{(1)}_{(g+nG)M+l} w_{m,l} \sum_{k=1}^{K}\sum_{q=0}^{1}\beta_k(q) \cdot \left[\lambda_c^{(k)}(g,l-1;n-qD/T\,|\,q)\bar{\eta}(\delta_k) + \lambda_c^{(k)}(g,l;n-qD/T\,|\,q)\bar{\eta}(T_c-\delta_k)\right]. \quad (39)$$

In the above, the complex envelope of the kth user's I/Q multicode signal is defined by $\lambda_c^{(k)}(g,l;n\,|\,q) \triangleq \lambda_I^{(k)}(g,l;n\,|\,q) + j\lambda_Q^{(k)}(g,l;n\,|\,q)$ in which the envelope of per-channel multicode signal is given by $(A = I, Q, n_q = n + qD/T)$

$$\begin{aligned}\lambda_A^{(k)}(g,l;n\,|\,q) &= \sum_{m=0}^{M-1} d_{A,m}^{(k)}(n-\kappa_{g,l}) w_{m,[(g+\kappa_{g,l}G)M+l-\nu_k]} \\ &\quad\cdot b_{A,\langle m\rangle}^{(k)}(\lfloor((g+\kappa_{g,l}G)M+l-\nu_k)/M\rfloor; n-\kappa_{g,l}\,|\,q) \\ &\quad\cdot c^{(k)}_{(g+n_qG)M+l-\nu_k}. \end{aligned} \quad (40)$$

Here, $\kappa_{g,l} = \lfloor(gM+l-\nu_k)/N\rfloor$ for $\nu_k = \lfloor\tau_k/T_c\rfloor, [l] = l \operatorname{modulo} M$ and $\delta_k = \tau_k - \nu_k T_c$.

Then, the decision variable $\rho_{\langle m\rangle}(n;i,e)$ in (15) is expressed by $Z \triangleq \mathrm{Re}\{\rho_{\langle m\rangle}(n;i,e)\} = \sum_{k=1}^{K} Z_k$ where the kth user term Z_k is

$$\begin{aligned} Z_k = \frac{1}{2JN}\sum_{g=0}^{G-1}\sum_{l=0}^{M-1}\sum_{q=0}^{1} c^{(1)}_{(g+n_+G)M+l}\left(\alpha_i\cdot \mathbf{w}_{\langle m\rangle,l}\right) \\ \cdot h_{e+qG/2,g}\mathrm{Re}\{\beta_1^*(q)[\beta_k(0)\Gamma_k(g,l;n+qD/T\,|\,0) \\ +\beta_k(1)\Gamma_k(g,l;n-(1-q)D/T\,|\,1)]\} \end{aligned} \quad (41)$$

for $\Gamma_k(g,l;n\,|\,q) \triangleq \lambda_c^{(k)}(g,l-1;n\,|\,q)\bar{\eta}(\delta_k) + \lambda_c^{(k)}(g,l;n\,|\,q)\bar{\eta}(T_c-\delta_k)$ and $\mathbf{w}_{\langle m\rangle,l} = (w_{m',l},\ldots, w_{m'+J-1,l})$ $(m' = \langle m\rangle J)$.

From the Gram–Charlier series in [16], the p.d.f. $f_k(y)$ of $Y_k = Z_k/\sigma_{I,k}$ $(k \geq 2)$ has the form

$$f_k(y) = \phi(y) + \sum_{n=3}^{\infty} a_n \phi^{(n)}(y). \quad (42)$$

Since $\{Y_k\}$ is a set of zero-mean i.i.d. random variables, we obtain the characteristic function

$$\begin{aligned} C(j\omega) &\triangleq \mathbf{E}\left\{\exp\left(j\omega\sum_{k=2}^{K} Y_k\right)\right\} \\ &= \exp[-(K-1)\omega^2/2]\left[1+\sum_{n=3}^{\infty} a_n (j\omega)^n\right]^{K-1} \end{aligned} \quad (43)$$

Let us define $\mu_n = \mathbf{E}\{Y_k^n\} = \mathbf{E}\{Z_k^n\}/\sigma_{I,k}^n$ and then $\mu_n = 0$ for an odd number n, resulting in $a_n = 0$, where $\{c_l^{(k)}\}$ in (5) are modeled as random binary sequences. Hence, $C(j\omega)$ is simplified to

$$\begin{aligned} C(j\omega) = \exp[-(K-1)\omega^2/2][1 + a_4(K-1)(j\omega)^4 \\ + a_6(K-1)(j\omega)^6 + \cdots]. \end{aligned} \quad (44)$$

Taking the inverse Fourier transform of $C(j\omega)$ gives the p.d.f. of $U \triangleq \sum_{k=2}^{K} Y_k$

$$\begin{aligned} f(u) = \frac{1}{\sqrt{K-1}}\left[\phi\left(\frac{u}{\sqrt{K-1}}\right) + \frac{a_4}{(K-1)}\phi^{(4)}\left(\frac{u}{\sqrt{K-1}}\right)\right. \\ \left. \times + \frac{a_6}{(K-1)^2}\phi^{(6)}\left(\frac{u}{\sqrt{K-1}}\right) + \cdots\right]. \end{aligned} \quad (45)$$

Note that, as K increases, $f(u)$ converges to the Gaussian function, i.e., the sum is asymptotically Gaussian. Thus, $f(y)$ in (16)

is easily derived with the change of variable $Y = U\sigma_{I,k}$ because $\mathbf{E}\{Z\} = Z_1$ and $\sigma_I^2 = (K-1)\cdot\sigma_{I,k}^2$.

Now it remains to evaluate the coefficient a_4 in (16) that is [16]

$$a_4 = \frac{(\mu_4 - 3)}{4!}. \tag{46}$$

First, $\sigma_{I,k}^2 = \mathbf{E}\{Z_k^2\}$ is evaluated as

$$\sigma_{I,k}^2 = \frac{M}{JN}\sigma_\beta^2 \mathbf{E}\{\bar{\eta}^2(\delta_k)\}(|\beta_1(0)|^2 + |\beta_1(1)|^2) \tag{47}$$

where $\sigma_\beta^2 = \mathbf{E}\{|\beta_k(q)|^2\}$, and $(A = I, Q)$

$$\mathbf{E}\left\{\left(\alpha_i \cdot \mathbf{w}_{\langle m\rangle,l}\right)^2\right\} = J, \quad \mathbf{E}\left\{\left[\lambda_A^{(k)}(g,l;n\,|\,q)\right]^2\right\} = M. \tag{48}$$

After a few steps, the fourth-order moment $\mathbf{E}\{Z_k^4\}$ can be approximated to

$$\begin{aligned}\mathbf{E}\{Z_k^4\} \cong \frac{3}{4}\left(\frac{M}{JN}\right)^2 \sigma_\beta^4 [3(|\beta_1(0)|^4 + |\beta_1(1)|^4) \\ \cdot (\mathbf{E}\{\bar{\eta}^4(\delta_k)\} + \mathbf{E}\{\bar{\eta}^2(\delta_k)\bar{\eta}^2(T_c - \delta_k)\}) \\ + 8|\beta_1(0)|^2|\beta_1(1)|^2(\mathbf{E}\{\bar{\eta}^2(\delta_k)\})^2].\end{aligned} \tag{49}$$

In the above, we have used that

$$\begin{aligned}\mathbf{E}\{|\Gamma_k(g,l;n\,|\,q)|^2|\Gamma_k(g',l';n\,|\,q)|^2\} \\ = 8M[\mathbf{E}\{\bar{\eta}^4(\delta_k)\} + \mathbf{E}\{\bar{\eta}^2(\delta_k)\bar{\eta}^2(T_c - \delta_k)\}]\end{aligned} \tag{50}$$

where $gM + l \neq g'M + l'$, and $\mathbf{E}\{|\beta_k(q)|^4\} = 2\sigma_\beta^4$. Thus, $\mu_4 = \mathbf{E}\{Z_k^4\}/\sigma_{I,k}^4$ is calculated as

$$\begin{aligned}\mu_4 \cong (3/4)\cdot\left[\frac{3[|\beta_1(0)|^4 + |\beta_1(1)|^4]}{[|\beta_1(0)|^2 + |\beta_1(1)|^2]^2}\Delta\right. \\ \left. + \frac{8|\beta_1(0)|^2|\beta_1(1)|^2}{[|\beta_1(0)|^2 + |\beta_1(1)|^2]^2}\right].\end{aligned} \tag{51}$$

By taking the average, i.e., $\mathbf{E}\{|\beta_1(q)|^2\} = \sigma_\beta^2$ and $\mathbf{E}\{|\beta_1(q)|^4\} = 2\sigma_\beta^4$, it can be approximated to

$$\mu_4 \cong \frac{3}{2}\Delta + 1. \tag{52}$$

Substituting μ_4 into (46) yields a_4 in (18).

Next, consider the case without transmit diversity where the transmit power P is used per (code) channel, and hence Z_k in (41) includes only the $q = 0$ term with $2JN$ replaced by JN. Then, it follows that the second-order moment $\sigma_{I,k}^2$ is given by

$$\sigma_{I,k}^2 = \frac{2M}{JN}\sigma_\beta^2|\beta_1(0)|^2\mathbf{E}\{\bar{\eta}^2(\delta_k)\} \tag{53}$$

and the fourth-order moment becomes

$$\begin{aligned}\mathbf{E}\{Z_k^4\} \cong 12\left(\frac{M}{JN}\right)^2 \sigma_\beta^4|\beta_1(0)|^4 \\ \cdot [\mathbf{E}\{\bar{\eta}^4(\delta_k)\} + \mathbf{E}\{\bar{\eta}^2(\delta_k)\bar{\eta}^2(T_c - \delta_k)\}]\end{aligned} \tag{54}$$

which produce $\mu_4 \cong 3\Delta$ and also a_4 in (18).

Appendix B
Decision Statistics $\{\rho_r(i,e)\}$ in (20)

For more realistic V-path Rayleigh fading channel, $\rho_r(i,e)$ can be formulated as

$$\begin{aligned}\rho_r(i,e) \\ = \frac{1}{2JN}\sum_{g=0}^{G-1}\sum_{l=0}^{M-1}\sum_{q=0}^{1} c_{(g+n_qG)M+l}^{(1)}\left(\alpha_i \cdot \mathbf{w}_{\langle m\rangle,l}\right) \\ \times h_{e+qG/2,g}\cdot\sum_{k=1}^{K}\sum_{v=1}^{V}\sum_{v'=1}^{V}\mathrm{Re}\{\beta_{1,v}^*(q)[\beta_{k,v'}(0) \\ \times \Gamma_k(g,l;n+qD/T;v'\,|\,0) + \beta_{k,v'}(1)\Gamma_k(g,l; \\ n-(1-q)D/T;v'\,|\,1)]\} + N_r(i;e)\end{aligned} \tag{55}$$

where $\Gamma_k(g,l;n;v'\,|\,q)$ is the same as $\Gamma_k(g,l;n\,|\,q)$ with τ_k replaced by $\tau_{k,v'} - \tau_{k,v}$ (fixed v). Here, the desired signal $D_r(i,e)$ in (20) is equivalent to the case of $k = 1$ and $v' = v$, that is,

$$D_r(i,e) = \begin{cases} 1/2\sum_{v=1}^{V}|\beta_{1,v}(0)|^2 + |\beta_{1,v}(1)|^2, \\ \text{if } \mathbf{d}_{I,\langle m\rangle}^{(1)}(n) = \alpha_i, \mathbf{b}_{I,\langle m\rangle}^{(1)}(n\,|\,q) = \mathbf{h}_{e+qG/2} \\ -1/2\sum_{v=1}^{V}|\beta_{1,v}(0)|^2 + |\beta_{1,v}(1)|^2, \\ \text{if } \mathbf{d}_{I,\langle m\rangle}^{(1)}(n) = -\alpha_i, \mathbf{b}_{I,\langle m\rangle}^{(1)}(n\,|\,q) = \mathbf{h}_{e+qG/2} \\ 0, \qquad\qquad \text{otherwise}\end{cases} \tag{56}$$

where $\mathbf{d}_{I,\langle m\rangle}^{(1)}(n) = [d_{I,\langle m\rangle}^{(1)}(n),\ldots,d_{I,\langle m\rangle J+J-1}^{(1)}(n)]$ and $\mathbf{b}_{I,\langle m\rangle}^{(1)}(n\,|\,q) = [b_{I,\langle m\rangle}^{(1)}(0;n\,|\,q),\ldots,b_{I,\langle m\rangle}^{(1)}(G-1;n\,|\,q)]$.

The kth user interference term $I_r^{(k)}(i,e)$ in (20) equals the first term in (55) with fixed $k \geq 2$, while the self-noise $I_r^{(1)}(i,e)$ in the case of $k = 1$ and $v' \neq v$. Then, the second-order moment $\sigma_{I,k}^2 = \mathrm{var}\{I_r^{(k)}(i,e)\}$ $(k \geq 2)$ is evaluated as

$$\begin{aligned}\sigma_{I,k}^2 = \frac{M}{2JN}\left[\sum_{v=1}^{V}(|\beta_{1,v}(0)|^2 + |\beta_{1,v}(1)|^2)\right. \\ \left.\cdot\sum_{v'=1}^{V}\mathbf{E}\{|\beta_{k,v}(0)|^2 + |\beta_{k,v}(1)|^2\}\mathbf{E}\{\bar{\eta}^2(\delta_{k,v'})\}\right]\end{aligned} \tag{57}$$

where $\delta_{k,v'} = \tau_{k,v'} - \tau_{k,v} - \nu_{k,v'}T_c$ for $\nu_{k,v'} = \lfloor(\tau_{k,v'} - \tau_{k,v})/T_c\rfloor$ (fixed v). Hence, $\sigma_{I,1}^2$ is obtained from (57) by subtracting out the term $v' = v$ $(k = 1)$. The filtered background noise $N_r(i,e)$ becomes zero-mean Gaussian noise with variance $N_o[\sum_{v=1}^{V}|\beta_{1,v}(0)|^2 + |\beta_{1,v}(1)|^2]/(16E)$. Therefore, the effective SNR $\gamma \triangleq D_r^2(i,e)/\mathrm{var}\{N_r(i,e) + \sum_{k=1}^{K} I_r^{(k)}(i,e)\}$ reduces to (28) when $J = 4$ is considered for symbol detection. Note that γ here becomes an approximation under unequal average path powers.

With a constant envelope signaling, $\{\alpha_i\}$ is confined to the subset $\{\alpha_1 = (-1,-1,-1,1), \alpha_2 = (-1,-1,1,-1), \alpha_4 = (-1,1,-1,-1), \alpha_7 = (-1,1,1,1), \alpha_8 = (1,-1,-1,-1), \alpha_{11} = (1,-1,1,1), \alpha_{13} = (1,1,-1,1), \alpha_{14} = (1,1,1,-1)\}$ $(J = 4)$. By the antipodal signals $\{\alpha_i\}$ and the channel orthogonalization $\mathbf{h}_{e+qG/2}\cdot\mathbf{h}_{e'+q'G/2}^T = 0$ $(e \neq e'$ or $q \neq q')$, decision statistics $\{\rho_r(i,e)\}$ become a biorthogonal set under the operator $\mathbf{E}$, i.e., statistically.

APPENDIX C
DERIVATION OF THE P.D.F. $f(\psi)$ IN (32)

Let us define $\Psi = \Psi_0 + \Psi_1$, where $\Psi_q \triangleq \sum_{v=1}^{V} \beta_{1,v}^2(q)$ for $q = 0, 1$. Since $\{\Psi_q\}$ are independent of each other and each p.d.f. is found in (37), the characteristic function $\varphi(j\omega) \triangleq \mathbf{E}\{\exp(j\omega\Psi)\}$ becomes

$$\varphi(j\omega) = \varphi_0(j\omega) \cdot \varphi_1(j\omega) = \prod_{v=1}^{V} \frac{1}{\left[1 - j\omega\sigma_\beta^2(v)\right]^2} \tag{58}$$

where $\varphi_q(j\omega) \triangleq \mathbf{E}\{\exp(j\omega\Psi_q)\}$. By taking the inverse Fourier transform of (58), we derive

$$\begin{aligned} f(\psi) &= f_0(\psi) \otimes f_1(\psi) \\ &= \sum_{v=1}^{V}\sum_{v'=1}^{V} \frac{\pi_v \pi_{v'}}{\sigma_\beta^2(v)\sigma_\beta^2(v')} \int_0^{\psi} \exp\left[-u/\sigma_\beta^2(v)\right] \\ &\quad \cdot \exp\left[-(\psi - u)/\sigma_\beta^2(v')\right] du \end{aligned} \tag{59}$$

where $f_q(\psi)$ is the p.d.f. of Ψ_q, $\otimes$ denoting the convolution.

REFERENCES

[1] V. Tarokh, N. Seshadri, and A. R. Calderbank, "Space-time codes for high data rate wireless communication: Performance analysis and code construction," *IEEE Trans. Inform. Theory*, vol. 44, pp. 744–765, Mar. 1998.

[2] V. Tarokh, A. Naguib, N. Seshadri, and A. R. Calderbank, "Combined array processing and space-time coding," *IEEE Trans. Inform. Theory*, vol. 45, pp. 1121–1128, May 1999.

[3] P. E. Mogensen, "GSM base-station antenna diversity using soft decision combining on up-link and delayed-signal transmission on down-link," in *IEEE Proc. VTC'93*, May 1993, pp. 611–616.

[4] J. H. Winters, "The diversity gain of transmit diversity in wireless systems with Rayleigh fading," *IEEE Trans. Veh. Technol.*, vol. 47, pp. 119–123, Feb. 1998.

[5] S. M. Alamouti, "A simple transmit diversity technique for wireless communications," *IEEE J. Select. Areas Commun.*, vol. 16, pp. 1451–1458, Oct. 1998.

[6] V. Weerackody, "Diversity for the direct-sequence spread spectrum system using multiple transmit antennas," in *IEEE Proc. ICC'93*, May 1993, pp. 1775–1779.

[7] K. Rohani, M. Harrison, and K. Kuchi, "A comparison of base station transmit diversity methods for third generation cellular standards," in *IEEE Proc. VTC'99*, May 1999, pp. 351–355.

[8] M. Raitola, A. Hottinen, and R. Wichman, "Transmission diversity in wideband CDMA," in *IEEE Proc. VTC'99*, May 1999, pp. 1545–1549.

[9] R. Prasad, "An overview of multi-carrier CDMA," in *IEEE Proc. ISSSTA'96*, Sept. 1986, pp. 107–114.

[10] I. Chih-Lin and R. D. Gitlin, "Multi-code CDMA wireless personal communications networks," in *IEEE Proc. ICC'95*, June 1995, pp. 1060–1064.

[11] I. Chih-Lin, G. P. Pollini, L. Ozarow, and R. D. Gitlin, "Performance of multi-code CDMA wireless personal communications networks," in *IEEE Proc. VTC'95*, Apr. 1995, pp. 907–911.

[12] E. Dahlman *et al.*, "UMTS/IMT-2000 based on wideband CDMA," *IEEE Commun. Mag.*, vol. 36, pp. 70–80, Sept. 1998.

[13] J. G. Proakis, *Digital Communications*, 2nd ed. New York, NY: McGraw-Hill, 1989.

[14] D. I. Kim, "Multidimensional constant envelope signaling for high-rate multicode DS-CDMA," *IEEE Trans. Commun.*, to be published.

[15] J. Fuhl, J. P. Rossi, and E. Bonek, "High-resolution 3D direction-of-arrival determination for urban mobile radio," *IEEE Trans. Antennas Propagat.*, vol. 45, pp. 672–682, Apr. 1997.

[16] A. D. Whalen, *Detection of Signals in Noise*. New York, NY: Academic, 1971.

[17] A. J. Viterbi, "Very low rate convolutional codes for maximum theoretical performance of spread-spectrum multiple-access channel," *IEEE J. Select. Areas Commun.*, vol. 8, pp. 641–649, May 1990.

[18] J. M. Wozencraft and I. M. Jacobs, *Principles of Communication Engineering*. New York, NY: Wiley, 1965.

[19] *Handbook of Mathematical Functions*, M. Abramowitz and I. A. Stegun, Eds., National Bureau of Standards, Washington, DC, 1964.

[20] T. Wada, T. Yamazato, M. Katayama, and A. Ogawa, "A constant amplitude coding for orthogonal multi-code CDMA systems," *IEICE Trans. Fundam.*, vol. E80-A, pp. 2477–2484, Dec. 1997.

Dong In Kim (S'89–M'91) received the B.S. and M.S. degrees in electronics engineering from Seoul National University, Seoul, Korea, in 1980 and 1984, respectively, and the M.S. and Ph.D. degrees in electrical engineering from the University of Southern California (USC), Los Angeles, in 1987 and 1990, respectively.

From 1984 to 1985, he was with the Korea Telecommunication Research Center as a Researcher. During 1986–1988, he was a Korean Government Graduate Fellow in the Department of Electrical Engineering, USC. From 1988 to 1990, he was a Research Assistant at the USC Communication Sciences Institute. Since 1991, he has been with the University of Seoul, Seoul, Korea, where he is currently an Associate Professor of the Department of Electrical and Computer Engineering, leading the Wireless Communications Research Group. He was a Visiting Professor at the University of Victoria, Victoria, BC, Canada, during 1999–2000. He has given many short courses and lectures on the topics of spread-spectrum and wireless communications at several companies. He has performed research in the areas of packet radio networks and spread-spectrum systems since 1988. His current research interests include spread-spectrum systems, cellular mobile communications, indoor wireless communications, and wireless multimedia networks.

Dr. Kim has served as an Editor of the IEEE JOURNAL ON SELECTED AREAS IN COMMUNICATIONS *Wireless Communications Series* and also as a Division Editor of the *Journal of Communications and Networks*. He currently serves as an Editor for Spread Spectrum Transmission and Access for the IEEE TRANSACTIONS ON COMMUNICATIONS and as an Editor for the IEEE TRANSACTIONS ON WIRELESS COMMUNICATIONS.

Vijay K. Bhargava (S'70–M'74–SM'82–F'92) received the B.Sc., M.Sc., and Ph.D. degrees from Queen's University, Kingston, ON, Canada, in 1970, 1972, and 1974, respectively.

Currently, he is Professor of Electrical and Computer Engineering at the University of Victoria, Victoria, BC, Canada. He is a co-author of the book *Digital Communications by Satellite* (New York: Wiley, 1981) and co-editor of the book *Reed-Solomon Codes and Their Applications* (New York: IEEE Press, 1994). His research interests are in multi-media wireless communications.

Dr. Bhargava is very active in the IEEE and has served as President of the Information Theory Society (2000), Vice President for the Regional Activities Board (1994, 1995), and Director of Region 7 (1992, 1993). In 1996 he was nominated by the Board of Directors for the Office of IEEE President-Elect. He was Co-chair for IEEE ISIT'95, Technical Program Chair for IEEE ICC'99 and is the Chair of IEEE VTC'2002 Fall, to be held in Vancouver. He is a fellow of the B.C. Advanced Systems Institute, Engineering Institute of Canada (EIC) and the Royal Society of Canada. He is a recipient of the IEEE Centennial Medal (1984), IEEE Canada's McNaughton Gold Medal (1995), the IEEE Haraden Pratt Award (1999), the IEEE Third Millennium Medal (2000), and the IEEE Graduate Teaching Award (2002).